ARTICLE

Experimental Study of C_2Cl_3+NO_2 Reaction[†]

Tian-cheng Xiang, Kun-hui Liu, Hong-mei Su*

State Key Laboratory of Molecular Reaction Dynamics, Beijing National Laboratory for Molecular Sciences, Institute of Chemistry, Chinese Academy of Sciences, Beijing 100080, China

(Dated: Received on May 31, 2007; Accepted on July 15, 2007)

The free radical reaction of C_2Cl_3 with NO_2 was investigated by step-scan time-resolved FTIR (TR-FTIR) emission spectroscopy. Due to the vibrationally excited products of Cl_2CO, NO, and CO, strong IR emission bands were observed with high resolution TR-FTIR spectra. Four reaction channels forming C_2Cl_3O+NO, CCl_3CO+NO, CO+NO+CCl_3, and ClCNO+Cl_2CO were elucidated, respectively. Spectral fitting showed that the product CO was highly vibrationally excited with the nascent average vibrational energy of 60.2 kJ/mol. Possible reaction mechanism via intermediates $C_2Cl_3NO_2$ and C_2Cl_3ONO was proposed.

Key words: TR-FTIR, C_2Cl_3, Vibrational population, Reaction mechanism

I. INTRODUCTION

As the simplest alkenyl radical, the vinyl radical is regarded as the important intermediate in the combustion process of hydrocarbon [1-10]. NO_2 is the important pollutant produced from the hydrocarbon combustion process. The reaction of unsaturated hydrocarbon radicals with NO_2 molecule may play an important role in the hydrocarbon combustion process, such as retarding the formation of PAH compounds or soot and reducing the release of pollutants into atmosphere [11-13]. A limited number of studies have been done on the reaction of vinyl with NO_2 in experiment or theory [14-16]. By means of LIF spectroscopy, Huang *et al.* measured the rate constant to be $(1.8\pm0.05)\times10^{-11}$ cm^3/(molecule s) at room temperature [14]. Using a tubular flow reactor coupled to a photoionization mass spectrometer, Geppert *et al.* measured the rate constant for this reaction to be $(4.19\pm0.05)\times10^{-11}(T/300)^{-0.60\pm0.07}$ cm^3/(molecule s) [15]. In their experiment, the only reaction product observed in the vinyl radical reaction with NO_2 is NO. They also performed *ab initio* calculations and predicted the following possible reaction pathways.

C_2H_3+NO_2 → C_2H_3O (non-cyclic)+NO
$\triangle H$=−206.3 kJ/mol
→ C_2H_3O (cyclic)+NO
$\triangle H$=−80.8 kJ/mol
→ CH_3CO+NO
$\triangle H$=−269.8 kJ/mol
→ C_2H_2+HNO_2
$\triangle H$=−203.8 kJ/mol

These are in consistent with the unimolecular decomposition channels of the compound nitroethylene (CH_2CHNO_2) calculated by Gindulyte *et al.* using a variety of methods including MP2, MP4, G2, and DFT [16].

Similarly, the chlorinated vinyl radical, C_2Cl_3, should also be taken into consideration as a critical intermediate in the combustion of chlorinated hydrocarbons which generally releases bad atmospheric pollutants [17]. However, the reactions of C_2Cl_3 radicals has been rarely studied. As a serial work prior to this study, we have studied the reaction of C_2Cl_3 radical with O_2 both theoretically [18] and experimentally [19]. In this paper, we report our preliminary experimental investigation on the products and channels of reaction C_2Cl_3 radical with NO_2 by means of step-scan time-resolved Fourier transform infrared emission spectroscopy (TR-FTIR). TR-FTIR is an effective technique probing multiple IR-active reaction products in real time due to its multiplex advantage and nanosecond time resolution. By observing the vibrationally excited products from the time-resolved IR emission spectra, several reaction channels are identified and the product vibrational energy disposal is derived from the spectral fitting. The experimental characterization of the products, channels and product energy disposal is of great help to understand the reaction mechanism and therefore to gain insights into related realistic processes, i.e., the pollution forming mechanism involved in the combustion of chlorinated hydrocarbons which is the usual treatments of chemical wastes and plastic wastes.

II. EXPERIMENTS

The reaction products are monitored by step-scan, time-resolved Fourier transform emission spectroscopy [20]. This newly upgraded machine comprises a Nicolet Nexus 870 step-scan FTIR spectrometer, Lambda Physik (LPX305i) Excimer laser, a pulse generator

[†]Part of the special issue of "Cun-hao Zhang Festschrift"
*Author to whom correspondence should be addressed. E-mail: hongmei@iccas.ac.cn,

(Stanford Research DG535) to initiate the laser pulse and achieve synchronization of the laser with data collection, two digitizers (internal 100KHz 16-bit digitizer and external 100 MHz 14-bit GAGE 8012A digitizer) which offer fast time resolution and a wide dynamic range as needed, and a personal computer to control the whole experiment. The detector used in this experiment is a liquid nitrogen cooled InSb detector.

The reaction is initiated in a stainless steel flow reaction chamber. A pair of parallel multi-layer coated mirrors (reflectivity R>0.95 at 248 nm) reflect the UV laser beam multiple times to increase the photolysis zone. C_2Cl_3 radicals are generated by 248 nm photodissociation (100 mJ/(cm^2 pulse), 10 Hz repetition rate) of C_2Cl_4. Samples of 12.00 Pa C_2Cl_4 ($\geq$99%) and 69.32 Pa NO_2 ($\geq$99.5%) enter the flow chamber 1 cm above the photolysis beam via needle valves. The chamber is pumped by an 8 L/s mechanical pump and the stagnation pressure of the chamber is measured by a MKS capacitance manometer. The constant pressure of the sample is maintained by adjusting the pumping speed and the needle valves. Transient infrared emission is collected by a pair of gold-coated White-Cell spherical mirrors and collimated by a CaF_2 lens to the step-scan Fourier spectrometer (Nicolet Nexus 870). The spectrometer and the collimating tube are both flushed with N_2 to eliminate the environmental CO_2 absorption. The spectral resolution is set at 0.5 cm^{-1}, the best resolution attainable with this instrument.

III. RESULTS AND DISCUSSION

A. Photolytic source of C_2Cl_3 radicals

In this experiment, C_2Cl_3 radicals were generated by 248 nm KrF laser photolysis of C_2Cl_4. Laser fluence dependence of the product yields have been measured in the intensity range of 4.2 and 9.6 MW/cm^2. As shown in Fig.1, the slope of the fluence dependence is 1.2±0.2, which means that only one photon dissociation process exists.

The one photon photodissociation process of C_2Cl_4 molecules are expected to follow two pathways:

$$C_2Cl_4 \rightarrow C_2Cl_3+Cl$$
$$\rightarrow C_2Cl_2+Cl_2$$

Russell *et al.* observed the formation of both the photoproducts C_2Cl_3 and C_2Cl_2 [17], indicating that the two pathways are of equal importance.

Besides the radical C_2Cl_3, there exist some possible interfering photofragments, i.e. Cl atoms, Cl_2, and C_2Cl_2 molecules. The Cl atoms do not react with precursor or NO_2 within the time scale of measurements, i.e., about hundreds of μs [21-24]. The other photofragments, the chlorinated acetylene C_2Cl_2 and Cl_2 are stable molecules and simply do not react with NO_2 molecules. Therefore, all the co-existed photofragments Cl atoms, Cl_2 molecules and chlorinated acetylenes

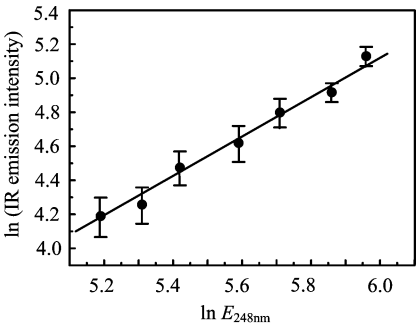

FIG. 1 Laser fluence dependence of the product IR emission signal with the slope of 1.2±0.2.

C_2Cl_2 are not likely to compete with the highly reactive C_2Cl_3 radicals in their reaction with NO_2 molecules. The photodissociation of C_2Cl_4 molecules provides a good source of C_2Cl_3 radicals.

B. Identification of reaction products and channels

In the first reference experiments of the pure photodissociation of C_2Cl_4, no transient IR emission signal was detected with the detector InSb because both of the IR-active photofragments C_2Cl_3 and C_2Cl_2 have vibrational frequencies below 1850 cm^{-1}, which is beyond the detection scope of InSb. When pure NO_2 was photolyzed by 248 nm laser, no IR emission signal was observed. Due to the small absorption cross section of NO_2 molecules at 248 nm (3.8×10^{-20} cm^2) [25], it is estimated that only a negligible amount (approximately 0.5%) of NO_2 molecules were dissociated at a laser power of 100 mJ/cm^2. As a result, no IR emissions due to the photofragments NO was observed in the TR-FTIR spectra.

Strong IR emission bands were observed upon the laser irradiation of the gas mixture of the C_2Cl_4 and NO_2 as shown in Fig.2, a series of TR-FTIR spectra at typical delay times from 5 μs to 120 μs after the initiation of the reaction by photolysis laser with a 0.5 cm^{-1} spectral resolution. These IR emissions arise from the vibrationally excited products of the reaction of C_2Cl_3+NO_2. Three emission bands were observed as shown in the 8 μs spectrum. Two rotationally resolved emission bands, the 2000-2250 cm^{-1} band and the 1850-1950 cm^{-1} band, are results of sets of ($v\rightarrow v-1$) rovibrational transitions of CO (v=1-9) and NO (v=1-3), respectively. The NO rovibrational lines are superimposed on top of an irresolvable emission band peak at 1850 cm^{-1}. According to its spectral position, this band is assigned to the polyatomic molecule Cl_2CO [19,26]. Because the detector InSb cuts off at 1850 cm^{-1}, only part of the emission bands of NO and Cl_2CO is detected in the spectra. All of these product IR emission signals appear in a few microseconds and grow to their maximum intensity roughly at 20 μs. The

DOI:10.1088/1674-0068/20/04/407-411

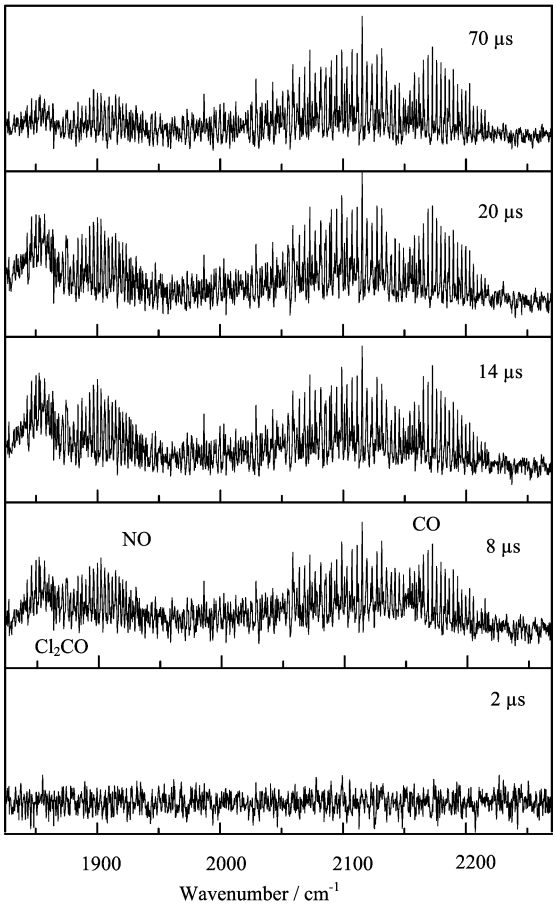

FIG. 2 TR-FTIR emission spectra of product from the reaction of C_2Cl_3+NO taken at representative reaction times from 2 μs to 70 μs with the spectral resolution of 0.5 cm^{-1}.

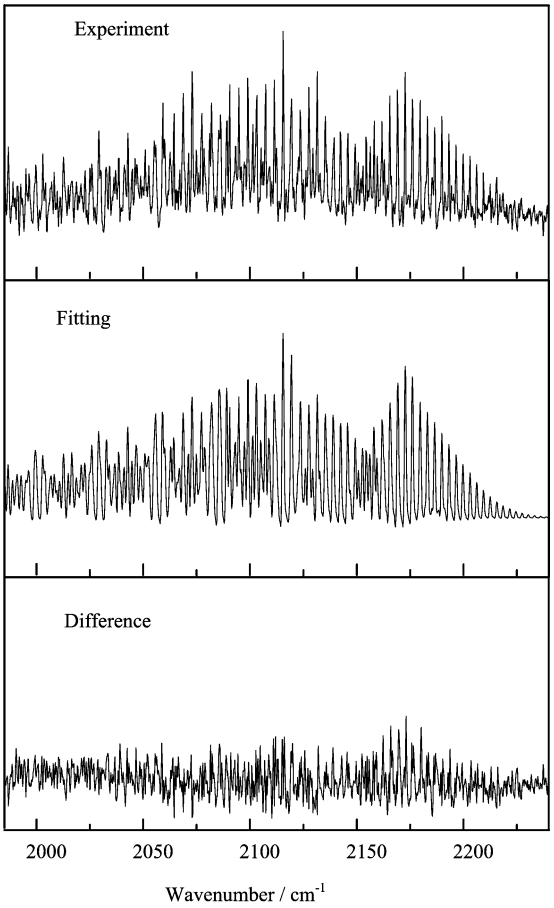

FIG. 3 Representative spectral fitting results for the IR emission band of the product CO collected at the reaction times of 16 μs. The difference between the experimental spectrum and the corresponding fitted spectrum is also shown at the bottom.

intensity of the Cl_2CO band decays rapidly due to fast vibrational energy transfer of polyatomic species and by the time 70 μs, it almost decreases to zero. In contrast, the other two diatomic species, CO and NO especially for CO, undergo slow vibrational energy transfer and thus their intensity sustains at longer delay times such as 70 μs.

By the above spectral assignments, the following reaction channels can be elucidated for the reaction of C_2Cl_3+NO_2:

$$C_2Cl_3+NO_2 \rightarrow C_2Cl_3O+NO \quad (1)$$
$$\triangle H=-239.6 \text{ kJ/mol}$$
$$\rightarrow CCl_3CO+NO \quad (2)$$
$$\triangle H=-154.3 \text{ kJ/mol}$$
$$\rightarrow CO+NO+CCl_3 \quad (3)$$
$$\triangle H=-170.1 \text{ kJ/mol}$$
$$\rightarrow ClCNO + Cl_2CO \quad (4)$$
$$\triangle H=-294.3 \text{ kJ/mol}$$

These channels are highly exothermic and thus lead to vibrationally excited products as observed in the IR emission spectra. The exothermicity of these channels is calculated using the heat of formation data in Ref.[27]. All of the reaction channels (1), (2), and (3) can contribute to the formation of the product NO, whereas the product CO or Cl_2CO corresponds to either channel (3) or channel (4), respectively.

C. Vibrational energy disposal of product CO

The vibrational energy disposal of the diatomic product CO are analyzed by fitting the IR spectra using a non-linear fitting program which has been described in details in Ref.[28]. For another diatomic product NO, spectral fitting is not performed simply because only part of its spectrum is observed with the detector InSb. Figure 3 shows the representative fitting results for the CO spectra collected at the time of 16 μs. Both of the rotational line positions and intensities fit well with the experimental spectra.

By spectral fitting, the vibrational populations of CO are derived to be 1, 0.32, 0.16, 0.11, 0.07, 0.06, 0.04, 0.03, 0.02 for the vibrational levels of v=1-9, respectively. As shown in Fig.4, the vibrational population

DOI:10.1088/1674-0068/20/04/407-411

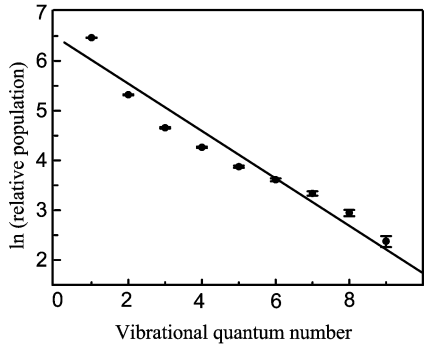

FIG. 4 Representative Boltzmann plot of the vibrational distribution of CO from the C_2Cl_3+NO_2 reaction at the reaction time of 16 μs. The straight line is the best fit of the data to a Boltzmann distribution with a temperature of 7700±900 K.

can be described nicely by a Boltzmann distribution with a vibrational temperature of $T_{\rm vib}$=7700±900 K. The corresponding average vibrational energy is thus calculated to be 56.8 kJ/mol.

Similarly, we fit the CO emission bands and derive the CO vibrational state distribution at different delay times. It is found that at all times, the product CO shows Boltzmann vibrational distribution. The corresponding average vibrational energy of CO at different reaction time of 8, 16, 20, 40, and 70 μs is 60.2, 56.8, 55.6, 54.3, and 53.5 kJ/mol, respectively. Apparently, the average vibrational energy of CO does not alter much with time, indicating that CO undergoes slow vibrational relaxation. This is due to the inefficient vibrational energy dissipation of CO molecules [29]. The colliding bath molecules NO_2 and C_2Cl_4 in the system do not have any vibrational modes in resonance with the CO stretching (2140 cm^{-1}). Although roughly 60 collisions (under total pressure of 81.3 Pa) occurs within 8 μs, the earliest time to observe descent signal, the average vibrational energy obtained at this time, 60.2 kJ/mol, should be very close to the nascent vibrational energy of CO. Divided by the available energy of the reaction channel (3) which generates CO, it is found that approximately 35% of energy is released as the CO vibrational energy. If assuming the internal energy of the other two accompanied products NO and CCl_3, substantial energy partition into the product internal degrees of freedom is expected.

The rotational temperature of 300 K always generates the best fitting results indicating that the rotational excitation has been thermalized. This is reasonable because these spectra are acquired as early as 8 μs, corresponding to roughly 60 collisions, which is sufficient to quench rotational excitation but not to alter the nascent vibrational excitation yet.

D. Possible reaction mechanism

Calculated at the MP2/6-311+G(d,p) level of theory [15], the C_2H_3+NO_2 reaction is revealed to proceed through three major intermediates nitroethylene ($C_2H_3NO_2$) and two vinyl nitrite isomers (C_2H_3ONO). The N-site attack of NO_2 is favored and thus the nitroethylene is initially formed with association energy of 313.6 kJ/mol. The energized nitroethylene can surmount the barrier rearranging to vinyl nitrite and subsequently decompose into the final products of C_2H_3O+NO. The nitro-nitrite rearrangements are found to be crucial in the mechanism.

In the present study for the reaction of C_2Cl_3+NO_2, similar mechanism can be proposed as shown in Fig.5. The reaction starts with the association of the C_2Cl_3 radical with NO_2 by the N-attack style forming C_2Cl_3-NO_2 and its subsequent isomerization to C_2Cl_3-ONO. The further dissociation of C_2Cl_3-ONO leads to the final products of C_2Cl_3O+NO. On the other hand, C_2Cl_3-ONO can rearrange to CCl_3CONO through a Cl atom migration and the further decomposition of CCl_3CONO forms eventually CCl_3CO+NO. The chlorinated acetyl radical CCl_3CO is highly unstable and expected to decompose further into CCl_3+CO.

The above proposed mechanism can explain well the reaction channels (1)-(3). For the reaction channel (4) generating the observed products Cl_2CO, more complicated mechanism is anticipated. To validate the feasibility of these channels and mechanism, detailed *ab initio* calculations are being performed. Interesting questions would arise such that if the nitro-nitrite rearrangements are also playing crucial roles in the reaction of C_2Cl_3+NO_2 and why substantial amount of energy is released as the internal excitation of the products. Combining the experimental findings with *ab initio* calculations, these questions are to be answered by further studies.

IV. CONCLUSION

In conclusion, for this free radical reaction of C_2Cl_3 with NO_2 which is of fundamental importance to atmospheric pollution process, we present the preliminary experimental results of the products, channels and vibrational energy disposal studied by step-scan TR-FTIR emission spectroscopy. Vibrationally excited reaction products of Cl_2CO, CO and NO are observed and four reaction channels forming C_2Cl_3O+NO, CCl_3CO+NO, CO+NO+CCl_3, and ClCNO+Cl_2CO, respectively, are therefore elucidated. Spectral fitting shows that the product CO is highly vibrationally excited with the nascent average vibrational energy of 60.2 kJ/mol. Possible reaction mechanism via intermediates $C_2Cl_3NO_2$ and C_2Cl_3ONO is proposed. These results can contribute to the understanding the pollution forming mechanism involved in the combustion of

DOI:10.1088/1674-0068/20/04/407-411

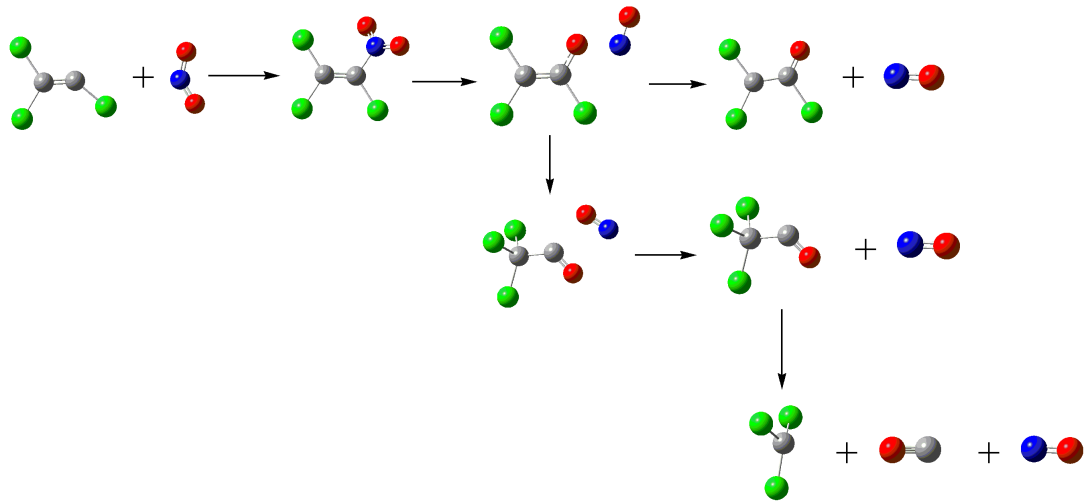

FIG. 5 Schematic diagram of the proposed reaction mechanism. The grey balls, green balls, red balls, and blue balls denote C atoms, Cl atoms, O atoms, and N atoms, respectively. For interpretation of the color in this figure legend, the reader can refer to the web version of this article.

chemical wastes and plastic wastes containing chlorinated hydrocarbons.

V. ACKNOWLEDGMENTS

We thank Professor Fan-ao Kong for constant encouragements and valuable discussions. This work was supported by the National Natural Science Foundation of China (No.20473100 and No.20673126) and Chinese Academy of Sciences.

[1] L. B. Harding, S. J. Klippenstein, and Y. Georgievskii, Proc. Combust. Inst. **30**, 985 (2005).
[2] A. H. Laufer and A. Fahr, Chem. Rev. **104**, 2813 (2004).
[3] D. L. Baulch, C. J. Cobos, R. A. Cox, C. Esser, P. Frank, T. Just, J. A. Kerr, M. J. Pilling, J. Troe, R. W. Walker, and J. Warnatz, J. Phys. Chem. Ref. Data. **21**, 411 (1992).
[4] Y. C. Wang, G. L. Dai, Z. Y. Geng, L. L. Lu, and D. M. Wang, Acta Phys. Chim. Sin. **20**, 1071 (2004).
[5] J. W. Bozzelli and A. M. Dean, J. Phys. Chem. **97**, 4427 (1993).
[6] A. m. Mebel, E. W. G. Diau, M. C. Lin, and K. Morokuma, J. Am. Chem. Soc. **118**, 9759 (1996).
[7] A. J. Eskola and R. S. Timonen, Phys. Chem. Chem. Phys. **5**, 2557 (2003).
[8] H. Krueger and E. Weitz, J. Chem. Phys. **88**, 1608 (1988).
[9] V. D. Knyazev and I. R. Slagle, J. Phys. Chem. **99**, 2247 (1995).
[10] A. Fahr and A. H. Laufer, J. Phys. Chem. **93**, 7229 (1988).
[11] D. C. Darwin and C. B. Moore, J. Phys. Chem. **99**, 13467 (1995).
[12] V. Seidler, F. Temps, H. G. Wagner, and M. Wolf, J. Phys. Chem. **93**, 1070 (1989).
[13] I. R. Slagle, F. Yamada, and D. Gutman, J. Am. Chem. Soc. **103**, 149 (1981).
[14] C. S. Huang, Z. Q. Zhu, Q. Ran, C. X. Chen, and Y. Chen, Acta Phys. Chim. Sin. **19**, 51 (2003).
[15] W. D. Geppert, A. J. Eskola, R. S. Timonen, and L. Halonen, J. Phys. Chem. A **108**, 4232 (2004).
[16] A. Gindulyte and L. Massa, J. Phys. Chem. A **103**, 11040 (1999).
[17] J. J. Russell, J. A. Seetual, D. Gutman, and S. M. Senkan, J. Phys. Chem. **93**, 1934 (1989).
[18] H. Wang, J. Li, X. Song, Y. Li, H. Hou, B. Wang, H. Su, and F. Kong, J. Phys. Chem. A **110**, 10336 (2006).
[19] T. C. Xiang, K. H. Liu, S. L. Zhao, H. M. Su, F. A. Kong, and B. S. Wang, J. Phys. Chem. A (accepted)
[20] P. W. Seakins, K. Liu, A. Wagner, *The Chemical Dynamics and Kineticss of Small Radicals*, Singapore: World Scientific, 250 (1995).
[21] W. B. DeMore, S. P. Sander, D. M. Golden, R. F. Hampson, M. J. Kurylo, C. J. Howard, A. R. Ravishankara, C. E. Kolb, and M. J. Molina, Jet Propulsion Laboratory Publication **97**, 1 (1987).
[22] R. Patrick and D. M. Golden, Int. J. Chem. Kinet. **15**, 1189 (1983).
[23] J. V. Seeley, J. T. Jayne, and M. J. Molina, J. Phys. Chem. **100**, 4019 (1996).
[24] A. R. Ravishankara, G. J. Smith, and D. D. Davis, Int. J. Chem. Kinet. **20**, 811 (1988).
[25] H. Okabe, *Photochemistry of Small Molecules,* New York: John Wiley & Son Inc., 271 (1978)
[26] A. H. Nielsen, T. G. Burke, P. J, H. Woltz, and E. A. Jones, J. Chem. Phys. **20**, 596 (1952).
[27] Y. R. Luo, *Handbook of Bond Energies,* Beijing: Science Press, (2005).
[28] H. Su, J. Yang, Y. Ding, W. Feng, and F. Kong, Chem. Phys. Lett. **326**, 73 (2000).
[29] V. Chikan and S. Leone, J. Phys. Chem. A **109**, 2525 (2005).

DOI:10.1088/1674-0068/20/04/407-411